Materials Advances

ROYAL SOCIETY OF CHEMISTRY

PAPER

View Article Online
View Journal | View Issue

Cite this: *Mater. Adv.*, 2025, **6**, 6406

Furanone-based comonomer used to manufacture antibacterial bone cement with simultaneously enhanced mechanical strength and antibacterial activity

Xin Wang,†[a] Wen-Han Bu,†[b] Lu-Yang Han,†[b] Long-Xu Han,[b] Qi-Ling Liang,[c] Shan He,[c] Zhe Gao,[d] Yang Xu,[c] Jian-Jun Chu*[bc] and Fang He*[ac]

Received 7th May 2025,
Accepted 3rd August 2025

DOI: 10.1039/d5ma00442j

rsc.li/materials-advances

Non-leaching bone cement (NLBC) with immobilized antibacterial agents represents a novel approach to fundamentally resolve the issue of burst release of antibiotic-loaded bone cement (ALBC). In this study, a furanone-based methacrylate carbamate comonomer has been reported, which we named FUMA. With this comonomer in hand, a new NLBC FUMA cement was manufactured. Surprisingly, the mechanical strength of the FUMA cement increased with the monomer content, meeting the ISO 5833 requirements. Further studies showed that the antibacterial activity of the FUMA cement increased with higher monomer content, and the 25% FUMA cement exhibited 97.57 ± 2.27% antibacterial activity against *Staphylococcus aureus* and 43 ± 4.82% against methicillin-resistant *Staphylococcus aureus* (MRSA). This cement demonstrated no hemolytic activity or acute toxicity. These findings provide new potential approaches for the prevention of periprosthetic joint infections (PJIs).

1 Introduction

With the intensification of population aging, the number of total joint replacements (TJRs) continues to rise, reaching millions of cases globally each year.[1,2] However, periprosthetic joint infections (PJIs) remain a frequent occurrence and have become one of the primary reasons for revision surgeries. To prevent PJIs, antibiotic-loaded bone cement (ALBC) is widely used in TJR.[3,4] Nevertheless, ALBC has several limitations, such as the degradation of mechanical properties, the burst release of antibiotics leading to toxicity, and the release of antibiotics below the minimum inhibitory concentration (MIC) after one week.[5,6] These issues may contribute to the inefficacy and lack of confidence in ALBC for PJIs prevention. Recent studies have also suggested that the effectiveness or cost-effectiveness of ALBC in preventing PJIs is suboptimal, likely due to these inherent drawbacks.[7–9]

In recent years, numerous innovative studies have been conducted to address these problems.[10–16] Among them, non-leaching bone cement (NLBC) with immobilized antibacterial agents represents a novel approach to fundamentally resolve the issue of burst release.[17–23] NLBC contains antibacterial groups that are either immobilized within the cement matrix or physically adsorbed, preventing their leaching. This shifts the antibacterial activity of NLBC from releasing antibacterial molecules into body fluids to contact killing, thereby eliminating the risk of burst release.[24–28] Research has primarily focused on two major classes of antibacterial motifs: quaternary ammonium salts and cyclic small molecules. Recently, heterocyclic structures such as furan and thiazole have garnered attention as antibacterial motifs. For example, Fu and Chu reported NLBC containing nitrofuran, while He reported benzothiazole-based NLBC. However, these NLBCs suffer from limitations such as insufficient mechanical strength or weak antibacterial activity, hindering further research and application. Our previous studies have shown that extending the chain length of monomers can effectively enhance mechanical strength.[17,21] Although this work has improved the mechanical strength of nitrofuran monomer-modified cement, it remains significantly below 70 MPa and fails to meet the ISO 5833 standard.

In this study, we designed and synthesized a novel furanone-based methacrylate carbamate comonomer, which we named

[a] *Department of Orthopedics, Hefei BOE Hospital, Teaching Hospital of Shanghai University Medical College, Hefei, Anhui 230013, China. E-mail: hefang8@126.com*
[b] *Department of Orthopedics, The Second People's Hospital of Hefei, Hefei Hospital, Affiliated to Anhui Medical University, No. 246 of Heping Road, Yaohai District, Hefei, Anhui 230011, China. E-mail: chujianj@mail.ustc.edu.cn*
[c] *Department of Pharmaceutical Science and Engineering, School of Food and Biological Engineering, Hefei University of Technology, Hefei, Anhui 230009, China. E-mail: xuyang@hfut.edu.cn*
[d] *Huaibei Miner General Hospital, Joint and Trauma Surgery, Huaibei, Anhui 235000, China*
† Xin Wang, Wen-Han Bu, Lu-Yang Han contributed equally to this work.

FUMA. This new monomer integrates three functional motifs: acrylic for polymerization, antibacterial furanone, and a long-chain linker enhancing mechanical stability. We hypothesize that this long-chain structure will promote mechanical strength. By incorporating FUMA into the liquid phase of bone cement, we develop a new type of NLBC, named FUMA bone cement. This study comprehensively evaluated FUMA cement's antibacterial activity, mechanical strength, and biocompatibility. Compared to existing ALBCs, FUMA cement demonstrates significant advantages in terms of preventing burst antibiotic release. Moreover, FUMA is the first monomer that simultaneously enhances the mechanical strength of cement and provides superior antibacterial activity both against *Staphylococcus aureus* and MRSA. This represents a new milestone in the field of advanced NLBCs reported to date. Its exceptional performance highlights its promising clinical application potential, offering new insights and pathways for the development and clinical practice in the field of orthopedics.

2 Materials and methods

2.1 Materials

PMMA bone cement (OSTEOPAL®V) and ALBC (PALACOS®R + G) were purchased from Heraeus Medical GmbH; 3,4-dichloro-5-hydroxyfuran-2(5*H*)-one (DHF) was sourced from Guangzhou Danao'an Biotechnology Co., Ltd; 2-isocyanatoethyl methacrylate (IEM) and dibutyltin dilaurate were obtained from Shanghai Aladdin Biochemical Technology Co., Ltd. Anhydrous sodium sulfate was purchased from Guangzhou Caisheng Biotechnology Co., Ltd; C57 mice were provided by the Animal Experiment Center of Anhui Medical University; MC3T3-E1 cells were sourced from Hunan Fenghui Biotechnology; reagents such as fetal bovine serum and trypsin were purchased from Bertin Instruments (USA); the CCK-8 kit was sourced from Beijing Transgen Biotech Co., Ltd; *Staphylococcus aureus* (ATCC 25923), MRSA (ATCC 43300) strains, clinical isolated multiple-resistant *Staphylococcus aureus* (hereafter referred to as clinical isolated MRSA; this strain is resistant to methicillin, various other antibiotics, and gentamicin; see Table S2 for details), centrifuges, CO_2 incubators, and clean benches were provided by the Clinical Laboratory of Hefei No. 2 People's Hospital; the MTS809 materials testing machine was provided by the University of Science and Technology of China; the spectrophotometer (Nanodrop One) was provided by the Central Laboratory of Anhui Medical University; reagents required for histological staining, including anhydrous ethanol, xylene, hematoxylin staining solution, eosin staining solution, as well as instruments such as a paraffin microtome and a tissue dryer, were provided by the Pathology Department of Hefei No. 2 People's Hospital.

2.2 Synthesis of FUMA comonomer

DHF (30 mmol, 1.0 equiv.) and IEM (36 mmol, 1.2 equiv.) were added to DCM (50 mL) and stirred thoroughly. Dibutyltin dilaurate (0.5 mL) was then added dropwise, and the mixture was stirred at room temperature for 3 hours. The reaction progress was monitored by thin-layer chromatography. After completion, the solvent was removed under reduced pressure at 40 °C using a rotary evaporator. The residue was dissolved in ethyl acetate (350 mL) and extracted with water (3 × 400 mL). The organic layer was dried over anhydrous sodium sulfate (200 g), and the solvent was removed by rotary evaporation at 50 °C. The crude product was purified by silica gel column chromatography to give the final product FUMA. The molecular design and synthesis route of FUMA are illustrated in Fig. 1. ^{1}H NMR (400 MHz, $CDCl_3$) δ 6.93–6.88 (m, 1H), 6.14 (d, J = 0.9 Hz, 1H), 5.65–5.60 (m, 1H), 5.45 (s, 1H), 4.37–4.18 (m, 2H), 3.64–3.49 (m, 2H), 1.95 (d, J = 1.0 Hz, 3H).

2.3 Preparation of FUMA bone cement

The formulations of bone cement at various concentrations are presented in Table 1. According to the concentrations, FUMA was weighed based on its mass ratio in the liquid phase and added to the liquid component of the bone cement. The mixture was thoroughly shaken to ensure complete dissolution, then combined with the solid phase of the bone cement and stirred evenly for 30 seconds. During the dough stage, the mixture was filled into molds. After complete hardening, the molds were removed to obtain cylindrical bone cement samples with a diameter of (6.0 ± 0.1) mm and a height of (12.0 ± 0.1) mm. These samples will be subjected to mechanical property and antibacterial activity studies. The bone cement saline extract and complete culture medium (containing 89% DMEM/F12 basic medium, 10% fetal bovine serum, and 1% penicillin–streptomycin antibiotic mixture) extract are obtained by soaking each type of bone cement in saline and complete culture medium respectively, at a ratio of 5 mL g^{-1}. The soaking process is conducted in a 37 °C, 5% CO_2 incubator with static conditions for 24 hours, followed by their use in leaching test and biocompatibility testing.

2.4 Characterization of FUMA bone cement

Fully mix PMMA cement and FUMA cement powders at concentrations of 5%, 15%, and 25% respectively with potassium bromide at a ratio of approximately 1 : 50. Grind the mixtures and then press them into pellets. Use Fourier Transform Infrared (FT-IR) spectrometer to record the prepared samples on a spectrophotometer (BRUKER VECTOR-22), with a frequency range of 4000–400 cm^{-1}. Utilize the software Origin to plot the FT-IR spectra.

2.5 Mechanical properties of FUMA bone cement

The synthesized PMMA cement and FUMA bone cement specimens of various concentrations (5 specimens per group) were polished with 1000-grit sandpaper to ensure parallelism of the top and bottom surfaces. After incubation at 37 °C and 100% humidity for 24 hours, the specimens were compressed using a computer-controlled materials testing machine (MTS809, Bose Corporation, USA) at a crosshead displacement rate of 20 mm min^{-1} under conditions of an ambient temperature of 24 ± 1 °C and a relative humidity of 40 ± 5%. Stress–strain

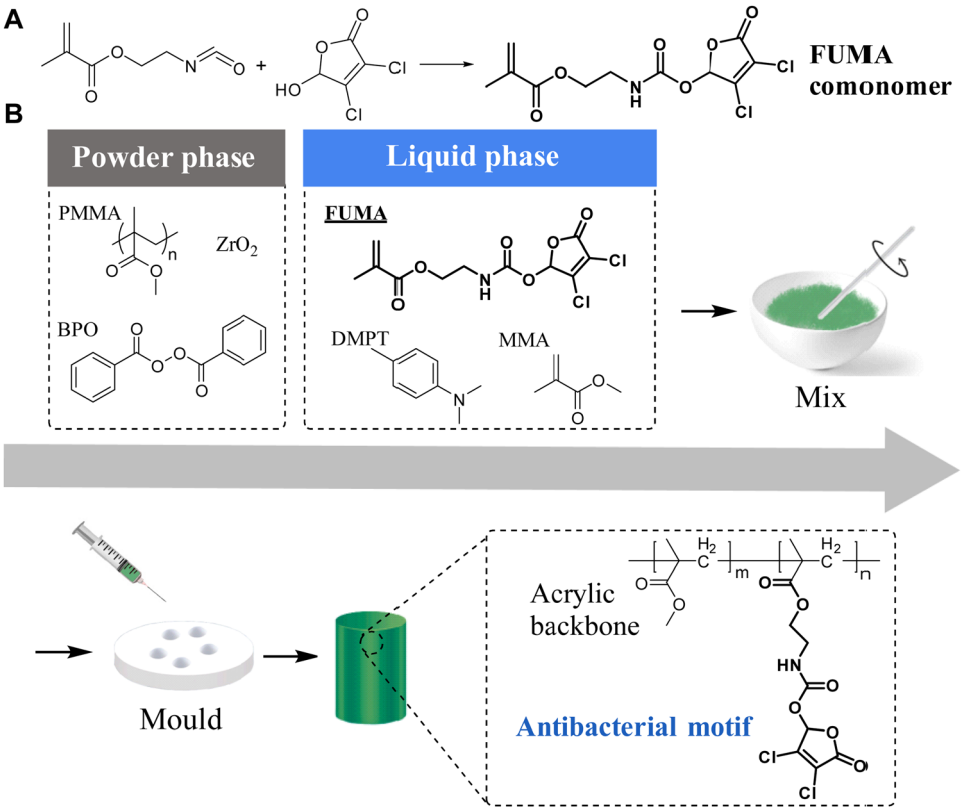

Fig. 1 (A) Synthetic route of FUMA (see Section 2.2 for details); (B) the FUMA cement was fabricated by mixing the solid phase with the liquid phase containing FUMA. The mixture was stirred until it reached the dough phase, then filled into the mold. After curing, the cement was removed from the mold.

Table 1 Formulation of PMMA bone cement and FUMA bone cement (percentage by mass of each component)

	Powder (%)			Liquid (%)		
Formulation	PMMA	ZrO_2	BPO	MMA	DMPT	FUMA
PMMA bone cement	34.83	28.71	0.24	35.43	0.77	0
5% FUMA bone cement	34.83	28.71	0.24	34.54	0.75	0.91
10% FUMA bone cement	34.83	28.71	0.24	33.66	0.73	1.81
15% FUMA bone cement	34.83	28.71	0.24	32.77	0.71	2.72
20% FUMA bone cement	34.83	28.71	0.24	31.89	0.69	3.62
25% FUMA bone cement	34.83	28.71	0.24	31.00	0.67	4.53

curves for each bone cement specimen were plotted. The compressive strength was obtained from the recorded stress–strain curves, and the elastic modulus was calculated based on the slope of the linear portion of the recorded stress–strain curves. Finally, the mechanical strength of the specimens in each group was evaluated according to ISO 5833 standards.

2.6 SEM of FUMA bone cement

Two square samples, each with a thickness of (2.0 ± 0.1) mm and a side length of (20.0 ± 0.2) mm, were prepared for PMMA bone cement, 5% FUMA bone cement, 25% FUMA bone cement, and ALBC (the formula of ALBC as shown in the Table S1). From each group, one sample was selected and soaked in physiological saline at 37 °C for 14 days. The prepared bone cement samples were subjected to brittle fracture in liquid nitrogen, followed by gold plating. Finally, SEM was used to observe the fracture surface morphology and assess the microstructural changes in the bone cement samples before and after soaking.

2.7 Evaluation of the antibacterial activity of FUMA bone cement

Contact antibacterial activity. Bone cement specimens were soaked in 3 mL of distilled water for 18 hours to remove unpolymerized FUMA monomers from the surface. A bacterial suspension with a concentration of (0.5×10^8) CFU mL^{-1} was prepared using resuscitated *Staphylococcus aureus* (ATCC 25923). Each bone cement specimen was immersed in 1 mL of the bacterial suspension and incubated in a 37 °C CO_2 incubator for 6 hours before being removed with sterile tweezers. The surface of the bone cement was then gently rinsed with 100 mL of distilled water to remove non-adherent bacteria. The bone cement specimens were then added to 5 mL of physiological saline and subjected to ultrasonic vibration for 3 minutes to dislodge bacteria adhering to the surface. Subsequently, the bone cement specimens were removed, and the remaining liquid was retained. From this liquid, 40 μL was diluted 100 times and thoroughly mixed. Then, 40 μL of the diluted bacterial suspension was evenly spread onto a bacterial culture plate. The plates were incubated in a CO_2 incubator at

37 °C for one day before counting. The antibacterial rate of bone cement containing different concentrations of FUMA was calculated using the following formula. Five replicate experiments were conducted for each concentration of bone cement.

$$\text{Antibacterial rate} = \frac{A - B}{A} \times 100\%$$

In the above equation, A represents the number of colonies on the Petri dishes with PMMA cement group, while B represents the number of colonies on the Petri dishes with different concentrations of FUMA bone cement group.

Leaching test. To compare with traditional ALBC and verify whether there is a release phenomenon in FUMA bone cement, we prepared 5 samples each of PMMA bone cement, 10% FUMA bone cement, 25% FUMA bone cement, and ALBC (the formula of ALBC as shown in the Table S1). Then, we prepared saline extracts of each group of bone cements. Subsequently, 1 mL of extract from each sample was mixed with 1 mL of *Staphylococcus aureus* suspension containing (0.5×10^8) CFU mL^{-1}. Meanwhile, a mixture of 1 mL of saline and 1 mL of bacterial suspension was prepared as the control group. All were incubated in a constant temperature incubator at 37 °C with 5% CO_2 for 24 hours. After thorough mixing, the obtained bacterial solution was diluted 2500 times and evenly spread onto Petri dishes. These were then incubated in a 37 °C incubator with 5% CO_2 for 1 day to count the bacterial colonies. By comparing the colony counts between the control group and the saline extracts of each group of bone cements, we evaluated the antibacterial effect of the saline extracts and verified whether FUMA bone cement exhibits release properties.

2.8 Determination of biocompatibility of FUMA bone cement

Hemolysis test. New Zealand white rabbits arterial blood was collected and centrifuged in a 10 mL centrifuge tube at 1000 rpm for 15 minutes. The supernatant plasma and other liquids were removed, and the precipitated red blood cells were resuspended in saline and centrifuged again at 1000 rpm for 15 minutes to further enhance purity. Finally, saline was added to prepare a 2% concentration of rabbit RBC suspension. The saline extracts of bone cement from various groups were mixed with the 2% rabbit red blood cell suspension at a ratio of 9 : 1 and incubated in an electromagnetic thermostat at 37 °C for 1 hour. The mixtures were then centrifuged at 3000 rpm for 5 minutes, and the supernatant was collected to measure its optical density (OD value) using a spectrophotometer. Simultaneously, OD values were measured for the negative control group (saline mixed at the same ratio) and the positive control group (pure water), based on which the hemolysis rates of the bone cement extracts of each group were calculated.

$$\text{Hemolysis rate} = \frac{OD_T - OD_N}{OD_p - OD_N} \times 100\%$$

In the above equation, OD_T represents the OD of the experimental group, OD_N represents the OD of the negative control group (saline), and OD_P represents the OD of the positive control group (distilled water).

Cytotoxicity test. The complete medium extracts of each group of bone cement were filtered and sterilized for later use. The resuscitated MC3T3-E1 cells were seeded into 96-well cell culture plates at a density of 5×10^3 cells per well, with 100 μL of complete medium pre-added to each well. After 24 hours, when the cells had adhered and stabilized, the medium was replaced with experimental group media containing 100 μL of the complete medium extracts of each group of bone cement. At the same time, a control group (complete medium) and a no-cell medium group were set up. After 1, 3, and 5 days of coculture, 10% volume of CCK-8 reagent was added to each well, and incubation was continued for 2 hours. The OD values were measured using a microplate reader at a primary wavelength of 450 nm and a reference wavelength of 630 nm. Three samples were prepared for each group of bone cement, and the experiment was repeated three times. The relative growth rate (RGR) of the cells was calculated using the following formula.

$$\text{RGR} = \frac{OD_{T'} - OD_R}{OD_{N'} - OD_R} \times 100\%$$

In the above equation, $OD_{T'}$ represents the OD of the experimental group, $OD_{N'}$ represents the OD of the control group (complete medium), and OD_R represents the OD of the cell-free medium.

Acute toxicity test in mice. Thirty-five 8-week-old male C57 mice were randomly divided into 7 groups, with 5 mice in each group. The experimental groups (saline extract of bone cement at various concentrations) and the control group (saline) were injected intraperitoneally into the C57 mice at a dose of 50 mL kg^{-1}. The mice were maintained under room temperature conditions with adequate food for 3 days before being euthanized, and their livers and kidneys were subsequently harvested. The mouse livers and kidneys were fixed in formalin solution for 1 day, followed by dehydration with ethanol, embedding in wax, sectioning, and drying. The sections were then stained with hematoxylin–eosin staining. By observing the liver and kidney sections and adhering to the guidelines of GB/T 16886, it was assessed whether the FUMA bone cement extracts induced acute toxicity in the mice.

2.9 Data statistics and analysis

The results obtained from the experiment were expressed in the form of mean ± standard deviation and the data were analyzed using the software SPSS 27. Statistical methods of one-way ANOVA and *post hoc* test of LSD were used for multiple comparisons to analyze the inhibition rate, mechanical strength, and hemolysis rate. The relative cell proliferation rate and in *vivo* acute toxicity test in mice were analyzed using repeated measures ANOVA and *post hoc* test of LSD. Statistical significance was defined with $p < 0.05$ indicating a significant difference and $p < 0.01$ indicating a highly significant difference.

3 Results and discussion

The FT-IR results for PMMA cement and FUMA bone cement with 5%, 15%, and 25% additions are presented in Fig. 2. These samples had the same signal peaks at 2950, 1730, 1244, and 1150 cm^{-1} that represented the characteristic peaks of the acrylic bone cement. Compared to PMMA cement, the FUMA cement exhibits a characteristic peak at 1810 cm^{-1} attributed to the C=O bond in the carbamate structure. As the amount of FUMA added increases, the intensity of this characteristic peak also increases. These results indicate that FUMA monomer was successfully incorporated into the cement.

The compressive strength of PMMA cement and FUMA bone cements are shown in the Fig. 3. Compared to PMMA cement, the compressive strength of 15% and 20% FUMA bone cement showed significant improvements ($p < 0.05$), while that of 25% FUMA bone cement exhibited highly significant improvement ($p < 0.001$). Additionally, 20% FUMA bone cement demonstrated significant enhancement in compressive strength compared to 5% and 10% FUMA bone cement ($p < 0.05$). The improvement in compressive strength of 25% FUMA bone cement was highly significant compared to 5% and 10% FUMA bone cement ($p < 0.001$), and also significant compared to 15% FUMA bone cement ($p < 0.05$). There were no significant differences among the other comparisons. The compressive strength of all bone cement groups met the requirements of the national standard ISO 5833, exceeding 70 MPa, and increased with higher concentrations. The elastic modulus of PMMA cement and FUMA bone cement at various concentrations are shown in the Fig. 4. In comparisons of elastic modulus, 20% FUMA bone cement showed significant improvement compared to PMMA cement and 10% FUMA bone cement ($p < 0.05$). Meanwhile, 25% FUMA bone cement demonstrated significant enhancement compared to PMMA cement, 5% FUMA bone cement, and 10% FUMA bone cement ($p < 0.05$). In our previous study on DHF–MAA bone cement,[23] high concentrations of DHF–MAA led to reduce the mechanical strength, potentially due to alkyl chains in the monomers weakening intermolecular forces, promoting molecular mobility, and affecting cement polymerization.[27] The FUMA in this study, compared to DHF–MAA which we previously reported, possesses longer side chain structures, which may result in smaller steric hindrance, thereby reducing their impact on the polymerization reaction.[21] These may be the reasons why the addition of FUMA monomer improves the mechanical properties. He reported a comonomer referred to as BTTMA, which, when added, can enhance the mechanical strength of bone cement; this constitutes a significant advancement in the field of NLBC.[29] Both FUMA and BTTMA are capable of improving the mechanical strength of bone cement, while the antibacterial activity of FUMA cement is superior to that of BTTMA cement. In conclusion, these results indicate that the FUMA bone cement has good mechanical properties.

The SEM images of PMMA bone cement, 5% FUMA bone cement, 25% FUMA bone cement, and ALBC before and after soaking are presented in Fig. 5 and 6. In the SEM images, we found that the fracture surfaces of all bone cements were

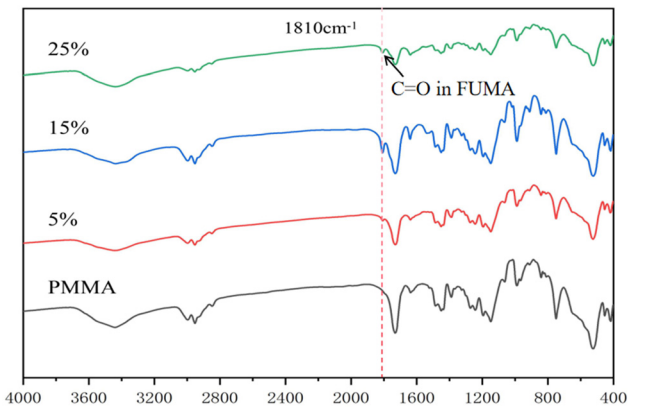

Fig. 2 FT-IR spectra of PMMA bone cement and FUMA bone cements.

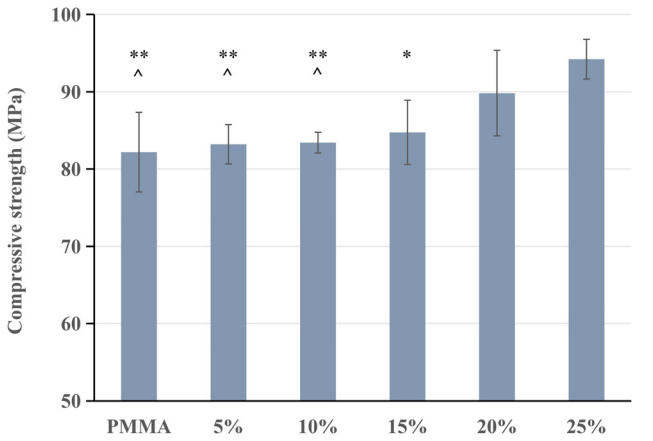

Fig. 3 Compressive strength of PMMA bone cement and FUMA bone cements (*. $p < 0.05$, indicates a significant difference compared to 25% FUMA bone cement, **. $p < 0.01$, indicates a highly significant difference. ^. $p < 0.05$, indicates a significant difference compared to 20% FUMA bone cement).

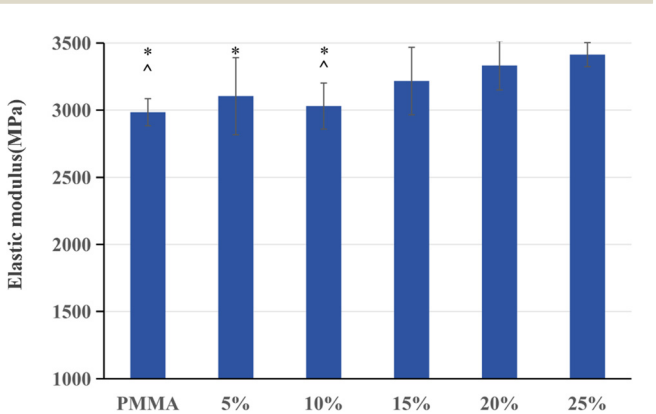

Fig. 4 Elastic modulus of PMMA bone cement and FUMA bone cements (*. $p < 0.05$, indicates a significant difference compared to 25% FUMA bone cement, ^. $p < 0.05$, indicates a significant difference compared to 20% FUMA bone cement).

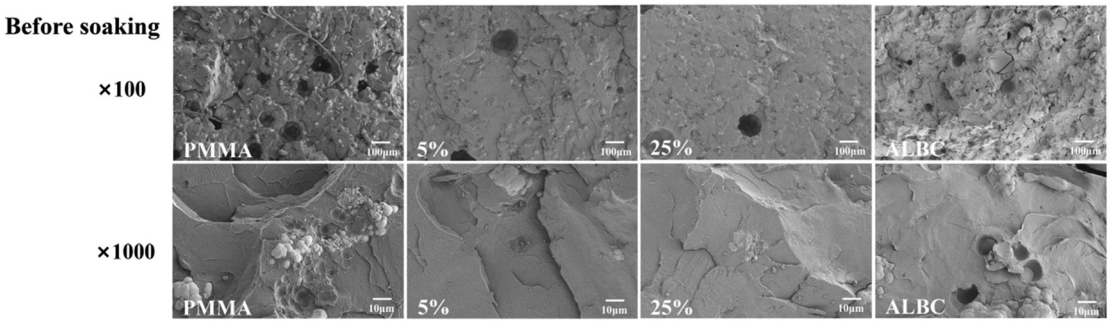

Fig. 5 SEM images at 100× and 1000× magnifications of PMMA bone cement, 5% and 25% FUMA bone cement, and ALBC before soaking.

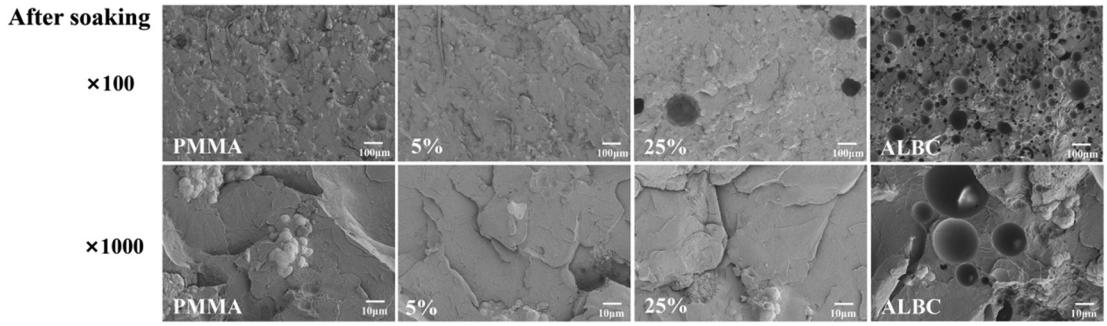

Fig. 6 SEM images at 100× and 1000× magnifications of PMMA bone cement, 5% and 25% FUMA bone cement, and ALBC after soaking.

uniform and dense before soaking, with some air bubbles formed during the mixing process of the bone cement. After soaking, there were no changes on the surfaces of PMMA and FUMU bone cements. Surprisingly, many small pores appeared on the fracture surface of the ALBC bone cement after soaking. We speculate that these pores were originally occupied by gentamicin, and they formed pores after the drug was eluted. These dense small pores are obviously different from the cavities formed by the air bubbles introduced during the mixing process. In Fig. S1 and S2, we provide SEM images of PMMA, all concentrations of FUMA cement, and ALBC at 100× and 1000× magnification. These results are similar to those of previous studies,[13] and indicate that the FUMA monomer has not been eluted. In addition, we provide more detailed SEM images of all bone cement before and after soaking at different magnifications for a more unambiguous representation (Fig. S3–S9).

The antibacterial activity of FUMA bone cement at various concentrations is illustrated in Fig. 7. In the surface antibacterial test, the antibacterial rate of 10% FUMA bone cement showed a significant increase compared to 5% FUMA bone cement ($p < 0.05$). The improvement in antibacterial rate for 15% FUMA bone cement was highly significant compared to both 5% and 10% FUMA bone cement ($p < 0.001$). Similarly, 20% FUMA bone cement demonstrated highly significant increases in antibacterial rate compared to 5% and 10% FUMA bone cement ($p < 0.001$), and a significant difference compared to 15% FUMA bone cement ($p < 0.05$). Notably, 25% FUMA bone cement exhibited highly significant increases in antibacterial rate compared to all other concentrations of FUMA bone cement (5%, 10%, 15%, and 20%) ($p < 0.001$). These results indicate a trend of increasing antibacterial rate with higher FUMA concentrations. We also observed a sharp increase in antibacterial rate when the concentration reached 25%, jumping from 47.60 ± 5.57% to 97.57 ± 2.27%. This may

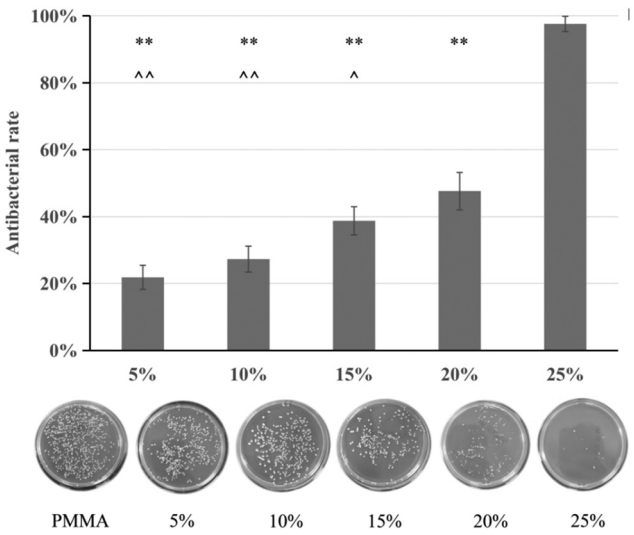

Fig. 7 Antibacterial rate of FUMA bone cements (**. $p < 0.01$, indicates a highly significant difference compared to 25% FUMA bone cement. ^. $p < 0.05$, indicates a significant difference compared to 20% FUMA bone cement, and ^^. $p < 0.01$, indicates a highly significant difference between 5% and 10%).

be related to the antibacterial mechanism of furanone motif, which is not fully understood but may include several aspects: furanone motif interfere with bacterial quorum sensing systems, inhibiting their communication signal molecules and thus preventing bacterial adhesion. Alternatively, furanone motif may induce the production of reactive oxygen species, leading to oxidative damage to bacterial cellular proteins and DNA, ultimately causing cell death.[30] Therefore, low-concentration FUMA bone cement samples allow some bacterial growth, whereas high concentrations exhibit high antibacterial activity. In order to further verify that the FUMA cement will not release antibacterial components, we carried out a leaching test. As shown in Table 2, different concentrations of FUMA bone cement, PMMA cement, and the control group all showed highly significant differences in colony counts compared to the ALBC group ($p < 0.001$). There were no statistical differences in antibacterial rates among the various concentrations of FUMA bone cement, PMMA cement, and the control group ($p > 0.05$). These results indicate that, similar to the drug-free PMMA cement, the FUMA cement does not release antibacterial components. In contrast, ALBC mainly relies on the release of antibiotics to kill bacteria, and this result is similar to that of the SEM analysis. Moreover, there have been few studies on the antibacterial activity of NLBC against drug-resistant bacteria. To confirm the boundaries of FUMA cement, we tested its antibacterial activity against MRSA. The results showed that 25% FUMA cement had 43 ± 4.82% antibacterial activity against MRSA (Fig. S10). In addition, to further explore the antibacterial activity of FUMA against MRSA, we tested the antibacterial activity of 20% and 25% FUMA cement against clinically isolated MRSA (Fig. S11). The antibacterial rate of FUMA against clinically isolated MRSA is lower than that against MRSA. FUMA belongs to non-leaching acrylic monomers and is a cyclic organic molecule. Although some progress has been made, its antibacterial mechanism remains unclear.[2] Overall, the study demonstrates that FUMA bone cement possesses decent antibacterial activity without leaching antibacterial agents.

We conducted hemolysis experiments with saline extracts of PMMA bone cement and FUMA bone cement at various concentrations. The observation results are shown in Fig. 8(A). It can be observed that, except for the positive control group, all the FUMA bone cement groups at various concentrations, the PMMA group, and the negative control group exhibited relatively clear and transparent liquids with no apparent differences and no hemolysis occurred. Furthermore, the supernatant after centrifugation was analyzed by using a spectrophotometer to determine its OD value, and the hemolysis rates of each group of bone cements were calculated as shown in Fig. 8(B). The experiments demonstrated that the hemolysis rates of the saline extracts of FUMA bone cement at all concentrations were less than 5%, and there was no statistically significant difference in hemolysis rates regarding the FUMA concentration ($p > 0.05$). However, we were puzzled why the hemolysis rate was not proportional to the amount of FUMA added, so we repeated the hemolysis experiment. The results are shown in Fig. S12, the hemolysis rates of all FUMA cements were below 5%, but the changing trend differed from that of the first experiment. The conclusion that the hemolysis rate was less than 5% in both tests was confirmable and reproducible, but the different trends observed in the experiments may be related to the experimental environment, blood batches, and operating techniques. Therefore, the experiments proved that FUMA bone cement does not cause hemolysis in rabbit red blood cells.

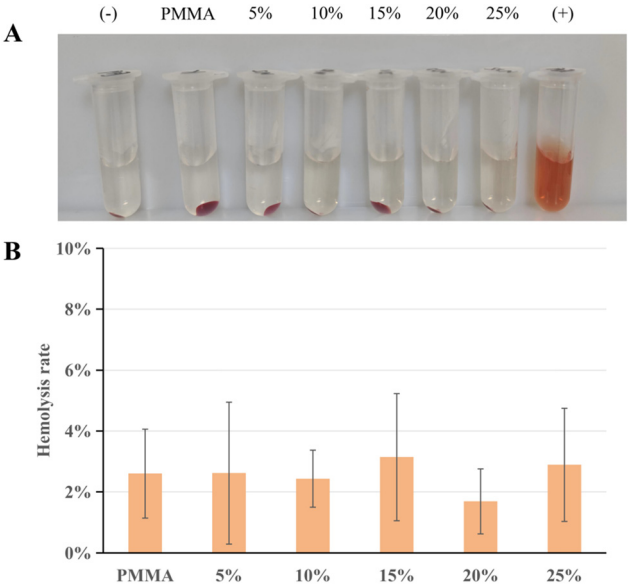

Fig. 8 (A) Hemolysis experiment for the PMMA bone cement, FUMA bone cements, negative control group (−), and positive control group (+); (B) hemolysis rates for the PMMA group and FUMA bone cement group.

Table 2 The colony count in the leaching test for normal saline (NS) group, PMMA bone cement group, 10% FUMA bone cement group, 25% FUMA bone cement group and ALBC group (*$p < 0.01$, indicates a highly significant difference compared to the NS group)

Group	Colony count
NS	357.8 ± 26.1
PMMA bone cement	337.4 ± 15.7
10% FUMA bone cement	339.4 ± 34.1
25% FUMA bone cement	336.6 ± 14.4
ALBC	4.8 ± 2.4*

The results of the RGR of FUMA bone cement at different concentrations, measured by the CCK-8 method, are presented in Fig. 9. Based on the analysis according to the GB/T 16886 standard, the RGR of all bone cement groups exceeded 75% in the first three days, indicating no cytotoxicity. However, on the fifth day, except for the control group, the RGR of all bone cement concentrations decreased compared to previous days ($p < 0.001$). The RGR of the PMMA bone cement group and the FUMA bone cement groups at various concentrations ranged between 50–75%, exhibiting mild cytotoxicity. The similar mild cytotoxicity observed in all groups except the control group may be attributed to the fact that the radiopaque agent (such as ZrO_2 used in the bone cement in this experiment) led to incomplete

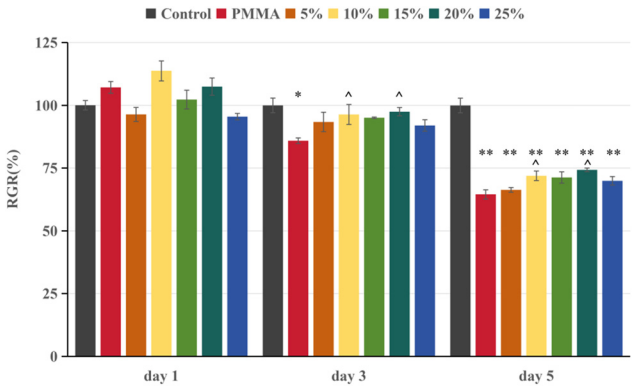

Fig. 9 RGR on the first day, third day, and fifth day for the control group, PMMA group, and FUMA bone cement group (*. $p < 0.05$, indicates a significant difference compared to the control group on the same day, **. $p < 0.01$, indicates a highly significant difference. ^. $p < 0.05$, indicates a significant difference compared to the PMMA group on the same day).

polymerization of some monomers and thus caused a certain degree of cytotoxicity.[31] Notably, on the fifth day of this experiment, the RGR of 10%, and 20% FUMA bone cement groups was statistically significantly increased compared to the PMMA bone cement group ($p < 0.05$). Therefore, we conclude that the addition of FUMA does not increase the cytotoxicity of the bone cement.

We further carried out an acute toxicity experiment, all mice showed no signs of coma, shock, vomiting, diarrhea, or other special symptoms during the injection of saline extracts from each group and in the following three-day observation period. Upon examination through HE staining (Fig. 10), it was found that the hepatic lobules and glomeruli of mice injected with saline, saline extracts of PMMA bone cement, and saline extracts of FUMA bone cement at various concentrations were all normal and undamaged, with no inflammatory cells or necrotic hepatocytes and renal cells observed in the field of view. Therefore, the result demonstrates that FUMA bone cement does not cause acute toxicity in mice.

4 Conclusions

We synthesized a novel furanone-based comonomer, called FUMA. This comonomer has a furan-based antibacterial motif which is connected to a methacrylate motif of the bone cement skeleton through a linker. Upon the addition of the FUMA, both the compressive strength and antibacterial activity of the bone cement were significantly enhanced. The 25% FUMA cement has 97.57 ± 2.27% antibacterial activity against *Staphylococcus aureus* and its compressive strength reaches 90 MPa. Further research has found that its antibacterial activity against MRSA reaches 43 ± 4.82%. At the same time, the FUMA cement has good biocompatibility, without hemolytic activity and toxicity to the liver and kidneys. All these findings indicate that the long-chain furanone based comonomer we designed can be used to fabricate high-performance antibacterial NLBC. This progress has increased the confidence and broadened the horizons for the clinical application of NLBC.

Ethics statement

The animal study was approved by this study was conducted with approval from the Biomedical Ethics Committee of Hefei University of Technology (no. HFUT20241025-002) and

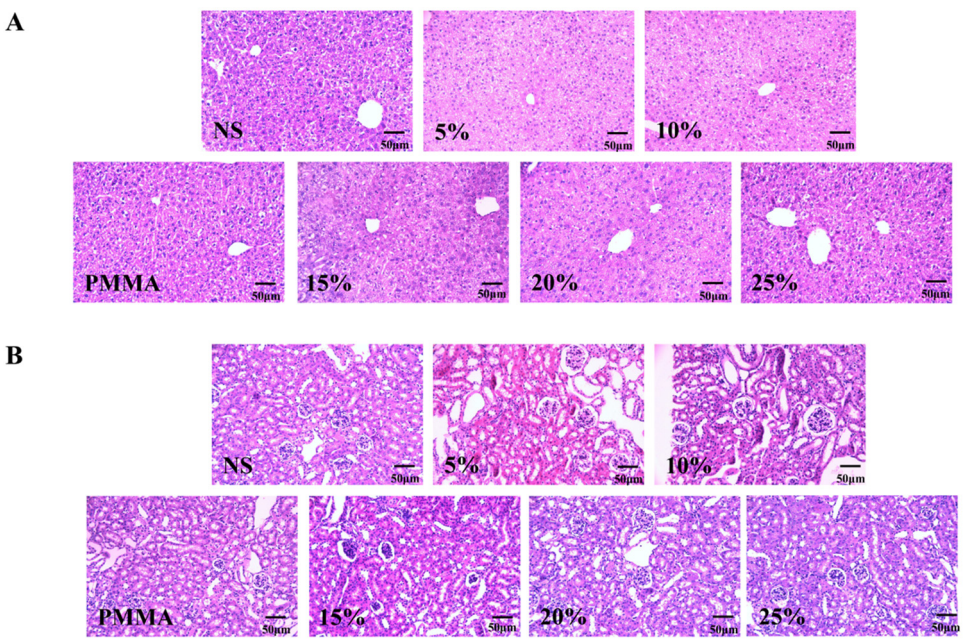

Fig. 10 (A) The liver sections of mice from the NS group, PMMA bone cement group, and FUMA bone cement group; (B) the kidney sections of mice from the NS group, PMMA bone cement group, and FUMA bone cement group.

complied with the National Institutes of Health Guide for the Care and Use of Laboratory Animals. This study was conducted in accordance with the declaration of Helsinki. The study was conducted in accordance with the local legislation and institutional requirements.

Author contributions

Conception and design of the research: Yang Xu, Jian-Jun Chu, Fang He. Acquisition of data: Wen-Han Bu, Lu-Yang Han, Xin Wang, Long-Xu Han, Qi-Ling Liang, Shan He. Analysis and interpretation of the data: Xin Wang, Wen-Han Bu, Lu-Yang Han, Yang Xu. Statistical analysis: Xin Wang, Wen-Han Bu, Lu-Yang Han, Yang Xu. Obtaining financing: Yang Xu, Jian-Jun Chu, Fang He. Writing of the manuscript: Wen-Han Bu, Xin Wang, Zhe Gao, Yang Xu. Critical revision of the manuscript: Yang Xu, Jian-Jun Chu, Fang He.

Conflicts of interest

The authors declare that the research was conducted in the absence of any commercial or financial relationships that could be construed as a potential conflict of interest.

Data availability

The original contributions presented in the study are included in the article/SI, further inquiries can be directed to the corresponding author.

Supplementary information is available. See DOI: **https://doi.org/10.1039/d5ma00442j**

Acknowledgements

This project was supported by the Health research Project of Anhui Province (AHWJ2024Ab0066, AHWJ2024Aa20414), and the Hefei Municipal Health Commission Applied Medical Project (Hwk2023zd011), and the Anhui Provincial Natural Science Foundation (2308085QB47).

References

1 V. J. Suhardi, D. A. Bichara, S. Kwok, A. A. Freiberg, H. Rubash, H. Malchau, S. H. Yun, O. K. Muratoglu and E. Oral, A Fully Functional Drug-Eluting Joint Implant, *Nat. Biomed. Eng.*, 2017, **1**, 0080, DOI: **10.1038/s41551-017-0080**.

2 H. Lin, Z. Gao, T. Shan, A. Asilebieke, R. Guo, Y. C. Kan, C. Li, Y. Xu and J. J. Chu, A review on the promising antibacterial agents in bone cement-From past to current insights, *J. Orthop. Surg. Res.*, 2024, **19**, 673, DOI: **10.1186/s13018-024-05143-7**.

3 J. Parvizi, K. J. Saleh, P. S. Ragland, A. E. Pour and M. A. Mont, Efficacy of antibiotic-impregnated cement in total hip replacement, *Acta Orthop.*, 2008, **79**, 335–341, DOI: **10.1080/17453670710015229**.

4 L. B. Engesaeter, B. Espehaug, S. A. Lie, O. Furnes and L. I. Havelin, Does cement increase the risk of infection in primary total hip arthroplasty? Revision rates in 56,275 cemented and uncemented primary THAs followed for 0-16 years in the Norwegian Arthroplasty Register, *Acta Orthop.*, 2006, **77**, 351–358, DOI: **10.1080/17453670610046253**.

5 A. Lilikakis and M. P. Sutcliffe, The effect of vancomycin addition to the compression strength of antibiotic-loaded bone cements, *Int. Orthop.*, 2009, **33**, 815–819, DOI: **10.1007/s00264-008-0521-3**.

6 J. Meyer, G. Piller, C. A. Spiegel, S. Hetzel and M. Squire, Vacuum-mixing significantly changes antibiotic elution characteristics of commercially available antibiotic-impregnated bone cements, *J. Bone Joint Surg. Am.*, 2011, **93**, 2049–2056, DOI: **10.2106/JBJS.J.01777**.

7 A. Pardo-Pol, A. Fontanellas-Fes, D. Pérez-Prieto, L. Sorli, P. Hinarejos and J. C. Monllau, The Use of Erythromycin and Colistin Cement in Total Knee Arthroplasty Does Not Reduce the Incidence of Infection: A Randomized Study in 2,893 Knees With a 9-year Average Follow-Up, *J. Arthroplasty*, 2024, **39**, 2280–2284, DOI: **10.1016/j.arth.2024.04.039**.

8 T. H. Leta, A. M. Fenstad, S. H. L. Lygre, S. A. Lie, M. Lindberg-Larsen, A. B. Pedersen, A. W-Dahl, O. Rolfson, E. Bülow, J. A. Ashforth, L. N. Van Steenbergen, R. G. H. H. Nelissen, D. Harries, R. De Steiger, O. Lutro, E. Hakulinen, K. Mäkelä, J. Willis, M. Wyatt, C. Frampton, A. Grimberg, A. Steinbrück, Y. Wu, C. Armaroli, M. Molinari, R. Picus, K. Mullen, R. Illgen, I. C. Stoica, A. E. Vorovenci, D. Dragomirescu, H. Dale, C. Brand, B. Christen, J. Shapiro, J. M. Wilkinson, R. Armstrong, K. Wooster, G. Hallan, J. E. Gjertsen, R. N. Chang, H. A. Prentice, E. W. Paxton and O. Furnes, The use of antibiotic-loaded bone cement and systemic antibiotic prophylactic use in 2,971,357 primary total knee arthroplasties from 2010 to 2020: an international register-based observational study among countries in Africa, Europe, North America, and Oceania, *Acta Orthop.*, 2023, **94**, 416–425, DOI: **10.2340/17453674.2023.17737**.

9 T. H. Leta, S. A. Lie, A. M. Fenstad, S. H. L. Lygre, M. Lindberg-Larsen, A. B. Pedersen, A. W-Dahl, O. Rolfson, E. Bülow, L. N. van Steenbergen, R. G. H. H. Nelissen, D. Harries, R. de Steiger, O. Lutro, K. Mäkelä, M. S. Venäläinen, J. Willis, M. Wyatt, C. Frampton, A. Grimberg, A. Steinbrück, Y. Wu, C. Armaroli, M. A. Gentilini, R. Picus, M. Bonetti, S. Dragosloveanu, A. E. Vorovenci, D. Dragomirescu, H. Dale, C. Brand, B. Christen, J. Shapiro, J. M. Wilkinson, R. Armstrong, K. Wooster, G. Hallan, J. E. Gjertsen, R. N. Chang, H. A. Prentice, A. Sedrakyan, E. W. Paxton and O. Furnes, Periprosthetic Joint Infection After Total Knee Arthroplasty With or Without Antibiotic Bone Cement, *JAMA Netw. Open*, 2024, **7**, e2412898, DOI: **10.1001/jamanetworkopen.2024.12898**.

10 L. Yang, A. A. Yergeshov, Y. Al-Thaher, S. Avdokushina, E. Statsenko, T. I. Abdullin and P. Prokopovich, Nanocomposite orthopaedic bone cement combining long-acting

dual antimicrobial drugs, *Biomater. Adv.*, 2023, **153**, 213538, DOI: 10.1016/j.bioadv.2023.213538.

11 Y. Al Thaher, R. Khalil, S. Abdelghany and M. S. Salem, Antimicrobial PMMA Bone Cement Containing Long Releasing Multi-Walled Carbon Nanotubes, *Nanomaterials*, 2022, **12**, 1381, DOI: 10.3390/nano12081381.

12 Y. Chen, G. Caneli and D. Xie, A PMMA bone cement with improved antibacterial function and flexural strength, *J. Biomater. Sci., Polym. Ed.*, 2022, **33**, 1398–1414, DOI: 10.1080/09205063.2022.2056943.

13 Y. Xu, H. Lin, Z. Gao, R. Guo, Y. C. Kan, L. Y. Han, W. H. Bu, Z. Wang, A. Asilebieke, L. X. Han, C. Li, F. He and J. J. Chu, Injectable isoniazid-loaded bone cement based on hydrazone bonds achieving long-term release and decent mechanical properties, *J. Mater. Chem. B*, 2024, **12**, 4389–4397, DOI: 10.1039/d3tb02661b.

14 Z. M. Wright, B. D. Holt and S. A. Sydlik, Covalently-controlled drug delivery via therapeutic methacrylic tissue adhesives, *J. Mater. Chem. B*, 2017, **5**, 7743–7755, DOI: 10.1039/c7tb01151b.

15 Z. M. Wright, A. M. Pandit, B. D. Holt and S. A. Sydlik, Therapeutic methacrylic comonomers for covalently controlled release from mechanically robust bone cement: Kinetics and structure–function relationships, *Macromolecules*, 2019, **52**, 3775–3786, DOI: 10.1021/acs.macromol.9b00368.

16 J. Singh, J. B. Mandell, J. Scheidt, J. D. Orlando, J. C. Kadir, W. B. Ribnick, K. M. Brothers, K. L. Urish and S. A. Sydlik, Antibiotic TMA (Therapeutic Methacrylic) Comonomers: Synergizing Mechanical Integrity with Infection Control in Bone Cement, *Adv. Funct. Mater.*, 2025, **35**, 2406126, DOI: 10.1002/adfm.202406126.

17 J. Chu, C. Li, J. Guo, Y. Xu and Y. Fu, Preparation of new bio-based antibacterial acrylic bone cement via modification with a biofunctional monomer of nitrofurfuryl methacrylate, *Polym. Chem.*, 2022, **13**, 4675–4683, DOI: 10.1039/D2PY00235C.

18 Z. Gao, Y. Xu, Y. Kan, H. Li, R. Guo, L. Han, W. Bu and J. Chu, Comparison of antibacterial activity and biocompatibility of non-leaching nitrofuran bone cement loaded with vancomycin, gentamicin, and tigecycline, *J. Orthop. Surg. Res.*, 2023, **18**, 569, DOI: 10.1186/s13018-023-04055-2.

19 Z. Gao, Y. C. Kan, Y. H. Xie, R. Guo, C. Li, A. Asilebieke, Y. Xu and J. J. Chu, A review on non-leaching antibacterial bone cement for orthopedic surgery: From past to current insights, *AIP Adv.*, 2023, **13**, 105034, DOI: 10.1063/5.0174845.

20 R. Guo, Y. C. Kan, Y. Xu, L. Y. Han, W. H. Bu, L. X. Han, Y. Y. Qi and J. J. Chu, Preparation and efficacy of antibacterial methacrylate monomer-based polymethyl methacrylate bone cement containing N-halamine compounds, *Front. Bioeng. Biotechnol.*, 2024, **12**, 1414005, DOI: 10.3389/fbioe.2024.1414005.

21 H. Lin, Z. Gao, L. Y. Han, J. J. Chu, Y. Xu and D. H. Shen, Antibacterial bone cement modified by long-chain nitrofuran methacrylate using liquid-phase modification strategy, *Front. Mater.*, 2024, **11**, 1432482, DOI: 10.3389/fmats.2024.1432482.

22 L. Y. Han, D. Yang, H. L. Wang, Z. Gao, Y. Y. Qi, Y. Zhou, Y. Xu and J. J. Chu, Bone cement prepared using the isobornyl acrylate monomer shows decent mechanical strength and antibacterial activity, *New J. Chem.*, 2025, **49**, 2106–2115, DOI: 10.1039/D4NJ04291C.

23 W. H. Bu, A. Asilebieke, L. Y. Han, Y. Xu, T. Zhou and J. J. Chu, Preparation and characterization of novel PMMA bone cement containing 3,4-dichloro-5-hydroxyfuran-2(5*H*)-one, *RSC Adv.*, 2025, **15**, 806–813, DOI: 10.1039/d4ra06607c.

24 S. Deb, R. Doiron, L. Disilvio, S. Punyani and H. Singh, PMMA bone cement containing a quaternary amine comonomer with potential antibacterial properties, *J. Biomed. Mater. Res., Part B*, 2008, **85**, 130–139, DOI: 10.1002/jbm.b.30925.

25 C. K. Abid, S. Jain, R. Jackeray, S. Chattopadhyay and H. Singh, Formulation and characterization of antimicrobial quaternary ammonium dendrimer in poly(methyl methcarylate) bone cement, *J. Biomed. Mater. Res., Part B*, 2017, **105**, 521–530, DOI: 10.1002/jbm.b.33553.

26 W. Zhu, F. Liu and J. He, Synthesis of imidazolium-containing mono-methacrylates as polymerizable antibacterial agents for acrylic bone cements, *J. Mech. Behav. Biomed. Mater.*, 2017, **74**, 176–182, DOI: 10.1016/j.jmbbm.2017.06.003.

27 W. Zhu, C. Lao, S. Luo, F. Liu, Q. Huang, J. He and Z. Lin, Mechanical and antibacterial properties of benzothiazole-based dental resin materials, *J. Biomater. Sci., Polym. Ed.*, 2018, **29**, 635–645, DOI: 10.1080/09205063.2018.1429861.

28 Y. Chen, G. Caneli and D. Xie, A PMMA bone cement with improved antibacterial function and flexural strength, *J. Biomater. Sci., Polym. Ed.*, 2022, **33**, 1398–1414, DOI: 10.1080/09205063.2022.2056943.

29 W. Zhu, F. Liu, B. Yu and J. He, Preparation of antibacterial acrylic bone cement with methacrylate derived from benzothiazole, *J. Mech. Behav. Biomed.*, 2021, **117**, 104403, DOI: 10.1016/j.jmbbm.2021.104403.

30 I. S. Sharafutdinov, A. S. Pavlova, F. S. Akhatova, A. M. Khabibrakhmanova, E. V. Rozhina, Y. J. Romanova, R. Fakhrullin, O. A. Lodochnikova, A. R. Kurbangalieva, M. I. Bogachev and A. R. Kayumov, Unraveling the Molecular Mechanism of Selective Antimicrobial Activity of 2(5*H*)-Furanone Derivative against *Staphylococcus aureus*, *Int. J. Mol. Sci.*, 2019, **20**, 694, DOI: 10.3390/ijms20030694.

31 P. Lopes, M. P. Garcia, M. H. Fernandes and M. H. Fernandes, Properties and osteoblast cytocompatibility of self-curing acrylic cements modified by glass fillers, *J. Biomater. Appl.*, 2013, **28**, 498–513, DOI: 10.1177/0885328212457097.